ACS Photonics

Letter

Cite This: ACS Photonics XXXX, XXX, XXX−XXX

Nonlinear Metasurface Based on Giant Optical Kerr Response of Gold Quantum Wells

Yuzhe Xiao,[†] Haoliang Qian,[†] and Zhaowei Liu*[,†,‡,§]

[†]Department of Electrical and Computer Engineering, University of California, San Diego, 9500 Gilman Drive, La Jolla, California 92093, United States

[‡]Material Science and Engineering, University of California, San Diego, 9500 Gilman Drive, La Jolla, California 92093, United States

[§]Center for Memory and Recording Research, University of California, San Diego, 9500 Gilman Drive, La Jolla, California 92093, United States

Supporting Information

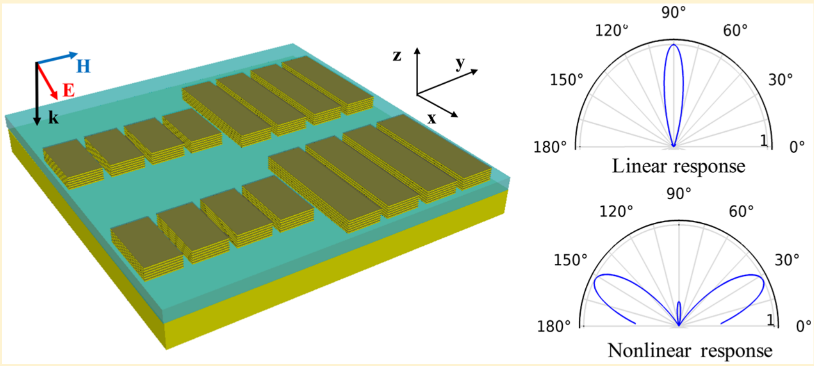

ABSTRACT: A nonlinear metasurface is demonstrated numerically based on the recently developed quantum-sized gold film. The active functionality of the metasurface is realized by varying the incident optical power through the ultrahigh Kerr nonlinearity of the quantum-sized gold films. In the low power region, the device acts as a normal reflecting surface, while it becomes a phase grating with most energy in the ±1 diffraction modes when the optical power increases and the nonlinear effect plays a dominating role. Unlike previously demonstrated nonlinear metasurfaces focusing on nonlinear frequency generation, the functionality of our device may be modulated by the power of incident light. As the first nonlinear metasurface that is based on optical Kerr nonlinearity, our design may lead to various applications, such as optical limiters and tunable phase gratings.

KEYWORDS: *metasurface, Kerr nonlinearity, gold quantum wells, phase grating*

Made by artificial materials with subwavelength thickness, a metasurface[1] can be thought of as the reduced dimensional version of a 3D metamaterial.[2] Being able to realize the same or even better functionalities of many bulky optical components but with a much smaller device thickness is the major motivation for extensive investigations of metasurfaces.[3,4] Since the work of the generalized law of reflection and refraction,[5] the field of metasurfaces has experienced a rapid growth. Different metasurfaces with specific functionalities have been demonstrated, such as flat lenses,[6] mirrors with anomalous reflection,[7] gratings,[8] and polarization convertors.[9] It is highly desirable for these ultrathin devices to be active and tunable for certain applications.[10,11] One of the approaches to achieve active functionality is to include nonlinearity into metasurface design.[12] By either using the nonlinearity of the plasmonic material itself[13,14] or incorporating high-nonlinear material such as semiconductor quantum wells combined with an existing plasmonic metasurface structure,[15,16] many nonlinear metasurfaces have been demonstrated recently. However, most of the nonlinear metasurfaces demonstrated so far are focused on the second-harmonic generation through the second-order nonlinearity.[13−16] A metasurface that can directly modulate the fundamental frequency of light itself through optical Kerr nonlinearity has not been demonstrated so far, due to limited third-order nonlinearity in existing materials.

Recently, an ultrathin metal film was demonstrated to have a giant optical Kerr nonlinear response due to the quantum confinement effect.[17] A quantum-sized gold film is a very promising material for nonlinear metasurfaces due to its giant optical nonlinearity as well as the fact that it is also a plasmonic material. In this Letter, we propose a nonlinear metasurface design that is based on such quantum-sized gold films. The active functionality is made possible through the ultrahigh

Special Issue: Ultra-Capacity Metasurfaces with Low Dimension and High Efficiency

Received: September 28, 2017
Published: February 7, 2018

DOI: 10.1021/acsphotonics.7b01140
ACS Photonics XXXX, XXX, XXX−XXX

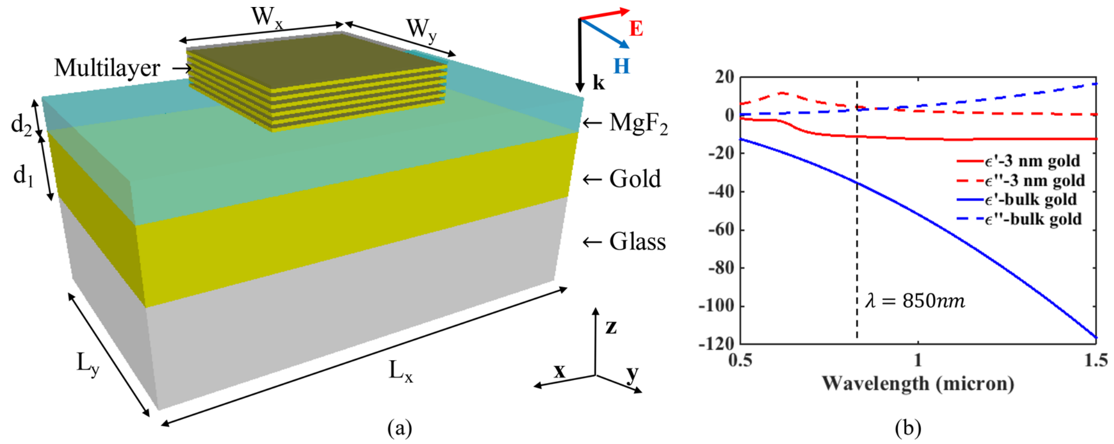

Figure 1. (a) Schematic of a building block of the nonlinear metasurface. The whole structure sits on a glass substrate, which is made of a top multilayer nanostructure and a bottom bulk gold layer separated by a MgF_2 spacer. (b) Permittivity (solid and dashed lines for real and imaginary parts, respectively) for 3 nm gold (red) and bulk gold (blue).

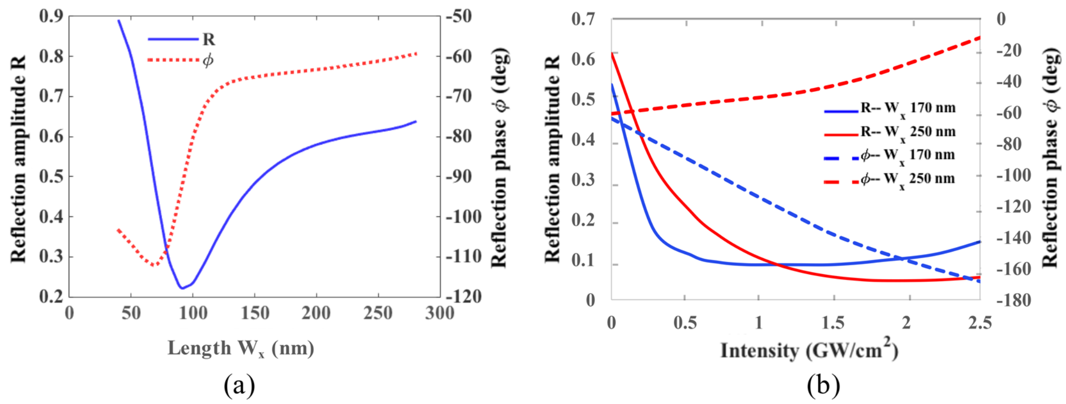

Figure 2. (a) Linear reflection coefficient $R = |r|^2$ (solid blue line) and the corresponding reflection phase ϕ (dotted red line) for the structure shown in Figure 1(a) with different particle length W_x. (b) Changes in R (solid line) and ϕ (dotted line) with different incident light intensity for an individual plasmonic structure with W_x = 170 nm (blue) and 250 nm (red), respectively.

optical Kerr nonlinearity. The device behaves as a normal reflecting surface that reflects incident light in the linear region, while it becomes a phase grating in the nonlinear region so that most of the reflected light is directed into the ±1 diffraction orders with the 0 order largely depressed. Our proposed metasurface is probably the first nonlinear metasurface that is based on Kerr optical nonlinearity and may lead to a variety of applications, such as optical power limiters.[18]

Figure 1(a) shows the basic structure that the nonlinear metasurface is built on. Sitting on a glass substrate, the whole structure consists of a Au-SiO_2 multilayer nanostructure on top and a thick gold film on the bottom, separated by a MgF_2 dielectric layer. The top multilayer nanostructure is made of six layers of Au (3 nm thick) and SiO_2 (2 nm thick), with a total thickness of 30 nm. Note that similar structures with different geometrical parameters have been demonstrated to exhibit different optical properties, such as a perfect plasmonic absorber[19] and an anomalous reflection mirror.[7] Here, the important difference of our structure is replacement of the top bulk gold particles with quantum-sized Au-SiO_2 multilayer nanostructures.

The thickness of each of the top gold layers is only 3 nm, in which the quantum confinement effect becomes critical. As a consequence, both the linear and nonlinear material properties of quantum-sized gold films show drastic differences as compared to those of the bulk gold.[17,20] Figure 1(b) compares the linear permittivity $\epsilon = \epsilon' + i \times \epsilon''$ for the 3 nm gold film (red lines, obtained experimentally from an identical gold−SiO_2 multilayer) and bulk gold (blue lines, from Johnson and Christy[21]).

The more relevant aspect here is the nonlinear properties. For existing metasurfaces made of noble metals, such as gold and silver, usually the intrinsic nonlinear response of metal is used.[13,14] Indeed, gold has a relatively large nonlinear response,[22] as compared to other conventional nonlinear materials.[23] However, its nonlinear response is still not high enough to achieve a sufficiently strong nonlinear effect within a deep subwavelength scale. Under this context, the quantum-sized gold film would be a promising candidate for a nonlinear metasurface, as it has been recently demonstrated that a 3 nm gold film has a giant third-order optical Kerr nonlinear response, which is about 4 orders higher than the intrinsic value of bulk gold.[17] As shown below, such a giant third-order nonlinear response enables the tunability of the metasurface with modest incident optical power.

The proposed structure shown in Figure 1(a) utilizes the response of the top nanostructure, as well as the coupling between the top and bottom metallic materials. The optical responses of the whole structure depend on the geometric parameters, as well as the material properties. Here we focus on

DOI: 10.1021/acsphotonics.7b01140
ACS Photonics XXXX, XXX, XXX−XXX

a structure with the fixed geometrical parameters $L_x = 300$ nm, $L_y = 120$ nm, $d_1 = 80$ nm, $d_2 = 50$ nm, and $W_y = 90$ nm and study its performance with respect to the length of the top nanostructure in the x-direction W_x at an exemplary wavelength of 850 nm. Simulations are performed using a finite element method (FEM) assuming a plane wave incident normally on the structure from the top with an electric field polarized along the x-direction. Figure 2(a) plots the reflection coefficient $R = |r|^2$ (solid blue line) and the corresponding phase ϕ (dotted red line) for the structure shown in Figure 1(a) with different length W_x. Due to the thick gold film at the bottom, transmission of the structure is almost zero. As can be seen here, there is an absorption peak around $W_x = 100$ nm, where reflection is minimized. Across the absorption peak, the reflection phase shows an almost linear dependence on the particle length. This length-dependent reflection phase feature has been utilized in a previous work to introduce a linear phase slope of the metasurface mirror to demonstrate anomalous reflection.[7]

Here we are more interested in the nonlinear response. From the third-order Kerr response, the refractive index of the 3 nm gold n (complex value) changes to the incident light intensity I following $n = n_0 + n_2 I$, where n_0 is the linear refractive index and n_2 is the Kerr coefficient.[23] Because of the intensity-dependent refractive index of the gold quantum well, the mode distribution of the plasmonic structure as well as the reflection amplitude R and phase ϕ change with incident optical power. Simulations are performed by varying the incident optical power for each specific top particle length W_x. Due to the giant Kerr coefficient of 0.2×10^{-8} cm^2/W of the 3 nm gold film near 850 nm,[17] this plasmonic structure shows a very large optical nonlinear response: both its reflection amplitude and phase can be changed by a large amount with modest incident optical power. Here we focus on two structures with $W_x = 170$ and 250 nm, which are shown to have a similar optical response in terms of reflection R and ϕ in the linear region, as depicted in Figure 2(a). Simulations are performed for these two structures with different incident optical intensities, and the corresponding R and ϕ are plotted in Figure 2(b) for incident light intensity up to 2.5 GW/cm^2. As shown here, the reflection coefficients R for both structures decrease from around 0.5 in the linear region to about 0.1 in the nonlinear region with an incident light intensity of 1.1 GW/cm^2. After 1.1 GW/cm^2, reflection increases slightly for $W_x = 170$ nm, while it is almost constant for $W_x = 250$ nm. The reflection phase, however, shows different behavior as I is increased: in the case of the 170 nm structure, ϕ decreases quickly from $-60°$ to about $-170°$, while it increases from $-60°$ to about $-10°$ for the case of the 250 nm structure.

With such a large nonlinear response, active nonlinear metasurfaces can be designed. Figure 3 shows the schematics for one of such examples. It is a periodic structure, with a single unit consisting of four repetitions of $W_x = 170$ nm elements, followed with another four repetitions of $W_x = 250$ nm elements. The period of the whole structure is 960 and 320 nm in the y- and x-direction, respectively. Other parameters are identical to the structure studied in Figure 2. In the linear region when the incident light intensity is weak, the reflection coefficients (both R and ϕ) of 170 and 250 nm elements are quite similar. Therefore, the whole structure essentially acts as a normal reflecting surface as seen by the incident light. With the increase of the incident light intensity, nonlinear effects become important. Although changes in the reflection coefficient R are very similar for the 170 and 250 nm elements (both decrease with I), changes in the reflection phase ϕ are in opposite directions, leading to a relative phase difference between them. For example, with an incident light intensity of 1.5 GW/cm^2, the relative phase difference between these two elements is about 90°. Such a structure is equivalent to a phase grating, with a modulation depth close to $\pi/2$. Therefore, one could expect such a metasurface to have different diffraction coefficients with different incident light intensities.

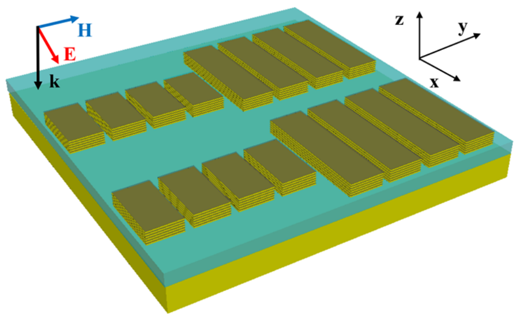

Figure 3. Schematics of a proposed nonlinear metasurface that consists of a periodic array of the plasmonic structures shown in Figure 1(a), with a single period consisting of four repetitions of $W_x = 170$ nm elements and four repetitions of $W_x = 250$ nm elements. The period in the y-direction is 960 nm, while it is 320 nm in the x-direction. Other parameters are identical to the structure studied in Figure 2.

To further demonstrate the performance of this nonlinear metasurface, a full simulation is performed using FEM. A plane wave is assumed to be incident normal to the structure from the top with the electric field polarized along the x-direction. Figure 4(a) and (b) plot the reflected electric field when the incident light intensities are 1 MW/cm^2 and 1.5 GW/cm^2, respectively. As can be seen here, when the incident light is very weak so that nonlinear effects can be neglected, the beam is reflected back in the normal direction. However, when the incident light intensity is high enough to induce a sufficient nonlinear material change, the reflected field shown in (b) is drastically different from the linear case shown in (a). The reflected field indicates an interference pattern with two waves propagating at opposite directions with respect to the surface normal.

To have a better understanding regarding the reflected field, the angular distributions of the reflected far field for both linear and nonlinear cases are plotted in polar plots in Figure 4(c) and (d), respectively. In the linear case, most of the light is reflected back in the normal direction (90°). The ±1 diffraction orders are negligibly small but still discernible due to the nonidentical responses from 170 and 250 nm elements. In the nonlinear case, most of the reflected light goes into two diffraction modes that propagate at about 30° and 150°, respectively, while the portion of light that is reflected normally backward is heavily suppressed. A series of simulations is performed by varying the incident light intensity I, where the ratio of the first- and zeroth-order diffraction mode energy is plotted in Figure 4(e). As can be seen here, the ratio is almost zero before 1 GW/cm^2 and then increases quickly and reaches a peak value of about 80 near 1.5 GW/cm^2, after which its value becomes smaller again. The reason for the decreased ratio is due to the relatively larger difference in reflection coefficient between the two units when intensity is sufficiently high, even though their phase response difference keeps increasing. Therefore, one can see that such a proposed metasurface in Figure 3 is indeed tunable: the relative

DOI: 10.1021/acsphotonics.7b01140
ACS Photonics XXXX, XXX, XXX−XXX

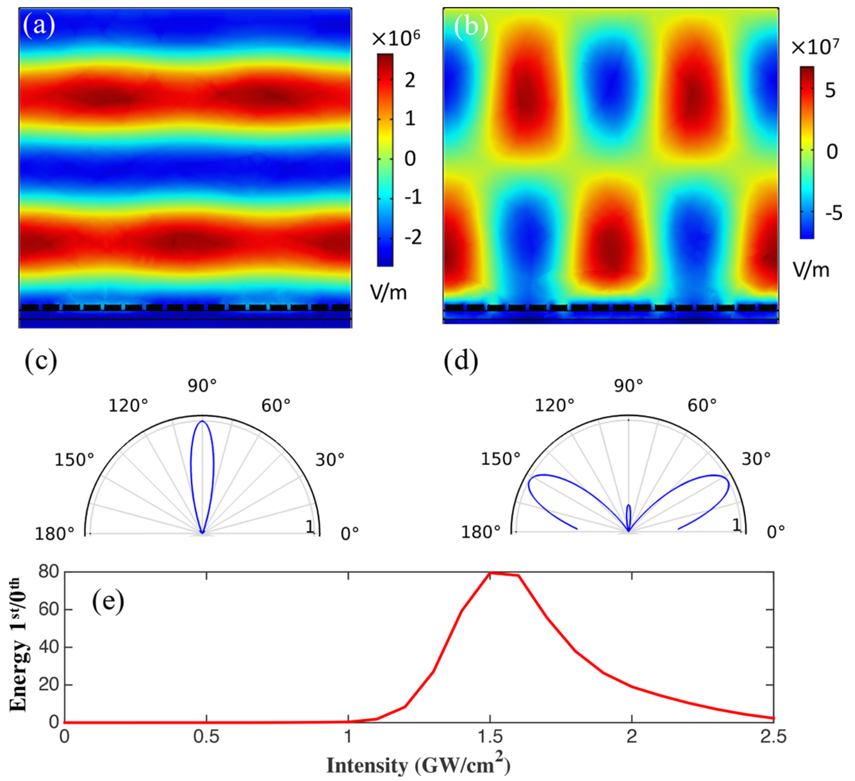

Figure 4. Simulated reflected electric field of the proposed nonlinear metasurface when the incident light intensity is weak, (a) $I = 1$ MW/cm^2, linear region, and strong, (b) $I = 1.5$ GW/cm^2, nonlinear region. The metasurface acts as a mirror that reflects light normally in the linear region, while it becomes a diffractive grating where most of the light is redirected into the ±1 diffraction orders when the 0 order is heavily depressed in the nonlinear region. The corresponding normalized angular distributions of the reflected far-field amplitude for linear and nonlinear cases are shown in (c) and (d), respectively. (e) Ratio of the first and zeroth order diffraction energy when the incident light intensity is varied.

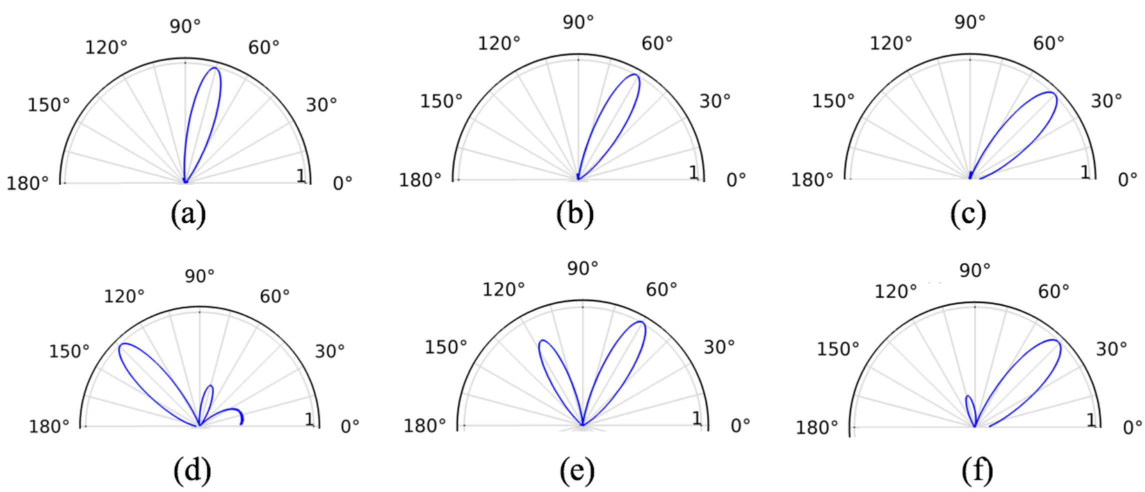

Figure 5. Calculated angular distributions of the reflected far field for linear ($I = 1$ MW/cm^2) cases with the incident angles of 15°, 30°, and 45° are shown in (a), (b), and (c), respectively. The corresponding nonlinear ($I = 1.5$ GW/cm^2) cases are shown in (d), (e), and (f), respectively.

amount of reflected light energy to different diffraction modes can be changed with incident optical power.

The proposed nonlinear metasurface also works for the case of oblique incident light. Figure 5 shows the calculated angular distributions of the reflected far field of the proposed device when the angle of incident light is 15°, 30°, and 45°. As can be seen from (a) to (c), the metasurface acts like a mirror with most of the energy going into the specular reflection angle when the incident light intensity is relatively small. When the incident light intensity becomes large, a significant amount of reflected energy goes into two ±1 diffraction orders. The performance of such an incident power dependent effect weakens as the incident angle becomes very large, as shown in Figure 5(d)−(f). Despite this, the proposed device works quite well for an incident angle within ±30°.

The fabrication of high-quality thin films with a thickness of a few nanometers is quite challenging. Two parameters are commonly used, i.e., average thickness and thickness variation, to describe the characteristics of practical films. In order to estimate the performance in a real device, we replace the ideally

DOI: 10.1021/acsphotonics.7b01140
ACS Photonics XXXX, XXX, XXX−XXX

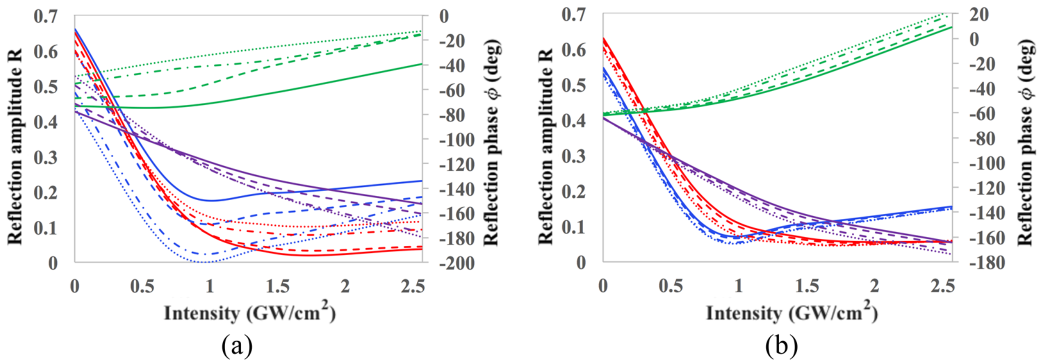

Figure 6. (a) Impact of a change in the gold layer thickness (solid line for 2 nm; dashed line for 2.5 nm; dash-dotted line for 3.5 nm; dotted line for 4 nm) on R (blue for W_x = 170 nm and red for W_x = 250 nm) and ϕ (purple for W_x = 170 nm and green for W_x = 250 nm), with the SiO_2 layer thickness fixed at 2 nm. (b) Same as (a) but with a different layer thickness for SiO_2 (solid line for 1 nm; dashed line for 1.5 nm; dash-dotted line for 2.5 nm; dotted line for 3 nm), with the gold layer thickness fixed at 3 nm.

uniform thin films of the top multilayer structure with randomly roughened surfaces with a thickness variation for each thin layer of 0.5 nm (Supporting Information Section 1), a typical value that has been achieved in our previously fabricated 3 nm gold films.[17] To consider the impact of uncertainty on average layer thickness, we performed a simulation by changing the gold layer and SiO_2 layer by ±0.5 nm and ±1 nm and plotted the results in Figure 6(a) and (b), respectively. Indeed, changing the thickness has an impact on both the reflection coefficient and reflection phase for the proposed plasmonic structure. Especially, the impact is relatively larger for the gold layer than that for the SiO_2 layer, which is not surprising since the nonlinear effect comes mainly from the metal films. In all cases, the phase difference between two individual elements increases from near 0° to almost 180° when the light intensity is increased to 2.5 GW/cm^2. We want to emphasize here that the simulation in Figure 6(a,b) only considers the impact of thickness variation on the plasmonic response of the proposed device. We assume the linear and nonlinear properties of all the gold films are the same as the 3 nm thick case. On the basis of these results, we postulate that all the phenomena discussed above should be valid in a practically achievable multilayer structure, although the exact power-dependent diffraction efficiency might be slightly different.

To conclude, we proposed a nonlinear metasurface based on the recently demonstrated ultrahigh optical Kerr nonlinearity of quantum-sized gold films. The optical functionality for such a metasurface can be controlled by the incident optical power. With a low incident optical power, the metasurface is a reflecting mirror, while it becomes a phase grating when the incident power is high enough and the nonlinear response becomes important. To our best knowledge, this is the first proposal of a nonlinear metasurface that is based on the third-order optical Kerr nonlinearity. The demonstrated nonlinear metasurface may find its usefulness in various nonlinear applications.

NUMERICAL METHOD

All electromagnetic simulations were performed with Comsol Multiphysics. Individual resonators were simulated with scattering periodic boundary conditions in the x- and y-direction. The resonator was excited with a plane wave from the top. The reflection coefficient (both amplitude and phase) is obtained via a global evaluation of the parameter S11. Resonator arrays (real metasurface) were simulated with periodic boundary conditions along the x- and y-directions. The angular distribution of the reflected field is from the far-field calculation.

Linear material properties of gold are chosen according to Figure 2(b), and the modeling of the nonlinear response of the gold layer is via

$$n = n_{\text{linear}} + \text{Re}\{n_2\}I$$

$$n = k_{\text{linear}} + \text{Im}\{n_2\}I$$

where $n_2 = 0.2 \times 10^{-8}$ cm^2/W is chosen from the experimental value measured at 850 nm.

ASSOCIATED CONTENT

Supporting Information

The Supporting Information is available free of charge on the ACS Publications website at DOI: 10.1021/acsphotonics.7b01140.

Additional information (PDF)

AUTHOR INFORMATION

Corresponding Author

*E-mail: zhaowei@ucsd.edu.

ORCID

Yuzhe Xiao: 0000-0002-0971-2480

Author Contributions

Y.X. and Z.L. conceived the concept. Y.X. and H.Q. performed the simulation. All authors wrote the manuscript. Z.L. supervised the research.

Notes

The authors declare no competing financial interest.

ACKNOWLEDGMENTS

This research is supported by the National Science Foundation, Division of Material Research (NSF-DMR-1610538).

REFERENCES

(1) Holloway, C. L.; Kuester, E. F.; Gordon, J. A.; O'Hara, J.; Booth, J.; Smith, D. R. An overview of the theory and applications of metasurfaces: The two-dimensional equivalents of metamaterials. *IEEE Antennas Propag. Mag.* **2012**, *54* (2), 10−35.

(2) Liu, Y.; Zhang, X. Metamaterials: a new frontier of science and technology. *Chem. Soc. Rev.* **2011**, *40* (5), 2494−2507.

(3) Kildishev, A. V.; Boltasseva, A.; Shalaev, V. M. Planar photonics with metasurfaces. *Science* **2013**, *339* (6125), 1232009.
(4) Yu, N.; Capasso, F. Flat optics with designer metasurfaces. *Nat. Mater.* **2014**, *13* (2), 139.
(5) Yu, N.; Genevet, P.; Kats, M. A.; Aieta, F.; Tetienne, J. P.; Capasso, F.; Gaburro, Z. Light propagation with phase discontinuities: generalized laws of reflection and refraction. *Science* **2011**, *334* (6054), 333−337.
(6) Aieta, F.; Genevet, P.; Kats, M. A.; Yu, N.; Blanchard, R.; Gaburro, Z.; Capasso, F. Aberration-free ultrathin flat lenses and axicons at telecom wavelengths based on plasmonic metasurfaces. *Nano Lett.* **2012**, *12* (9), 4932−4936.
(7) Sun, S.; Yang, K. Y.; Wang, C. M.; Juan, T. K.; Chen, W. T.; Liao, C. Y.; He, Q.; Xiao, S.; Kung, W. T.; Guo, G. Y.; Zhou, L. High-efficiency broadband anomalous reflection by gradient meta-surfaces. *Nano Lett.* **2012**, *12* (12), 6223−6229.
(8) Lin, D.; Fan, P.; Hasman, E.; Brongersma, M. L. Dielectric gradient metasurface optical elements. *Science* **2014**, *345* (6194), 298−302.
(9) Zhao, Y.; Alù, A. Manipulating light polarization with ultrathin plasmonic metasurfaces. *Phys. Rev. B: Condens. Matter Mater. Phys.* **2011**, *84* (20), 205428.
(10) Yao, Y.; Shankar, R.; Kats, M. A.; Song, Y.; Kong, J.; Loncar, M.; Capasso, F. Electrically tunable metasurface perfect absorbers for ultrathin mid-infrared optical modulators. *Nano Lett.* **2014**, *14* (11), 6526−6532.
(11) Zhu, B. O.; Chen, K.; Jia, N.; Sun, L.; Zhao, J.; Jiang, T.; Feng, Y. Dynamic control of electromagnetic wave propagation with the equivalent principle inspired tunable metasurface. *Sci. Rep.* **2015**, *4*, 4971.
(12) Minovich, A. E.; Miroshnichenko, A. E.; Bykov, A. Y.; Murzina, T. V.; Neshev, D. N.; Kivshar, Y. S. Functional and nonlinear optical metasurfaces. *Laser Photonics Rev.* **2015**, *9* (2), 195−213.
(13) Keren-Zur, S.; Avayu, O.; Michaeli, L.; Ellenbogen, T. Nonlinear beam shaping with plasmonic metasurfaces. *ACS Photonics* **2016**, *3* (1), 117−123.
(14) Almeida, E.; Shalem, G.; Prior, Y. Subwavelength nonlinear phase control and anomalous phase matching in plasmonic metasurfaces. *Nat. Commun.* **2016**, *7*, 10367.
(15) Lee, J.; Tymchenko, M.; Argyropoulos, C.; Chen, P. Y.; Lu, F.; Demmerle, F.; Boehm, G.; Amann, M. C.; Alu, A.; Belkin, M. A. Giant nonlinear response from plasmonic metasurfaces coupled to intersubband transitions. *Nature* **2014**, *511* (7507), 65.
(16) Nookala, N.; Lee, J.; Tymchenko, M.; Gomez-Diaz, J. S.; Demmerle, F.; Boehm, G.; Lai, K.; Shvets, G.; Amann, M. C.; Alu, A.; Belkin, M. Ultrathin gradient nonlinear metasurface with a giant nonlinear response. *Optica* **2016**, *3* (3), 283−288.
(17) Qian, H.; Xiao, Y.; Liu, Z. Giant Kerr response of ultrathin gold films from quantum size effect. *Nat. Commun.* **2016**, *7*, 13153.
(18) Hermann, J. A. Beam propagation and optical power limiting with nonlinear media. *J. Opt. Soc. Am. B* **1984**, *1* (5), 729−36.
(19) Hao, J.; Wang, J.; Liu, X.; Padilla, W. J.; Zhou, L.; Qiu, M. High performance optical absorber based on a plasmonic metamaterial. *Appl. Phys. Lett.* **2010**, *96* (25), 251104.
(20) Qian, H.; Xiao, Y.; Lepage, D.; Chen, L.; Liu, Z. Quantum electrostatic model for optical properties of nanoscale gold films. *Nanophotonics* **2015**, *4* (1), 413−418.
(21) Johnson, P. B.; Christy, R. W. Optical constants of the noble metals. *Phys. Rev. B* **1972**, *6* (12), 4370.
(22) Boyd, R. W.; Shi, Z.; De Leon, I. The third-order nonlinear optical susceptibility of gold. *Opt. Commun.* **2014**, *326*, 74−79.
(23) Boyd, R. W. *Nonlinear Optics*; Academic Press, 2007; Chapter 4.

DOI: 10.1021/acsphotonics.7b01140
ACS Photonics XXXX, XXX, XXX−XXX